PHILOSOPHICAL TRANSACTIONS OF THE ROYAL SOCIETY A MATHEMATICAL, PHYSICAL & ENGINEERING SCIENCES

On the Intrinsic Dynamics of Premixed Flames

G. I. Sivashinsky

Phil. Trans. R. Soc. Lond. A 1990 **332**, 135-148
doi: 10.1098/rsta.1990.0105

On the intrinsic dynamics of premixed flames

By G. I. Sivashinsky†

The Institute for Applied Mathematics and Scientific Computing, Indiana University, 618 E. 3rd Street, Bloomington, Indiana 47405, U.S.A.

[Plate 1]

A brief account of the structure and dynamics of freely propagating premixed gas flames in the régime of spontaneous flame instability is given. Recent theoretical studies providing a reduction of the pertinent free-boundary problem to a single evolution equation for the flame interface are discussed. The striking feature of the premixed flame is described. The flame, being an entirely deterministic system, proves capable of displaying irregular spatio-temporal behaviour similar to that known in hydrodynamic turbulence.

1. Introduction

The premixed flame (the self-sustained wave of exothermic chemical reaction) is the most natural mode of gaseous combustion and, hence, the main object of attention in combustion theory. Recently, however, premixed flames became of interest also to the general theory of dynamical systems. It transpires that flames, though fully deterministic physical systems, are, under certain conditions, liable spontaneously to become turbulent, as happens in flows of viscous fluid at large Reynolds numbers.

Although flame propagation is invariably accompanied by the motion of the underlying gaseous mixture, the nature of the flame generated turbulence is quite different from that of the viscous fluid, albeit sharing many of its basic features. For example, similar to the Navier–Stokes turbulence, flame dynamics involves many chaotic degrees of freedom. However, in contrast to the viscous fluid, flame turbulence may survive even in the one-dimensional version of the problem. In this sense the premixed flame provides a relatively simple yet quite realistic system for the study of turbulence-type phenomena, one of the most fascinating and challenging problems of nonlinear phenomenology (cf. Manneville 1988; Hohenberg & Shraiman 1989).

The present paper is intended as a wide-brush discourse on the inherent dynamics of flame propagation (rather an active topic in combustion theory). For a more systematic acquaintance with the fundamentals of the subject the reader may consult the recent monographs of Buckmaster & Ludford (1982), Strehlow (1984), Zel'dovich *et al.* (1980*a*), Williams (1985) and also surveys by Clavin (1985) and Sivashinsky (1983).

† Permanent address: Department of Mathematical Sciences, Tel Aviv University, Ramat Aviv, Tel Aviv 69978, Israel.

Phil. Trans. R. Soc. Lond. A (1990), **332**, 135–148 *Printed in Great Britain*

2. Experimental observations

The planar flame is clearly the most simple configuration of the combustion wave. While such flames are quite feasible in the laboratory, it is also known that under certain physico-chemical conditions flames spontaneously assume a more complex two- or three-dimensional structure.

It has long been known that the flame on a Bunsen burner may split up into triangular flamelets, which form, instead of the usual cone, a polyhedral pyramid that sometimes even rotates about its vertical axis (Smithells & Ingle 1882; Smith & Pickering 1928; figure 1, plate 1).

It was later found (Zel'dovich 1944; Markstein 1949) that this manifestation of spontaneous flame instability is not unique. In combustion in wide tubes (*ca.* 10 cm in diameter), the flame frequently breaks up into separate cells, *ca.* 1 cm in size, in a state of continuous irregular self-motion, merging and splitting (figure 2, plate 1).

It has been observed that the cellular instability primarily occurs in fuel–oxidizer mixtures that are deficient in the light reactants (e.g. rich mixtures of heavy fuels or lean mixtures of light fuels), i.e. when the Lewis number of the deficient reactant is smaller than some critical value.

However, as has also been noticed, although cells are reluctant to emerge in high Lewis number premixtures, the flames here are nevertheless not absolutely stable and may exhibit sharp wide-spaced ridges which are well maintained even under deformation and extension of the flame (Markstein 1964; Strehlow 1984). Moreover, in experiments with spherical flames propagating in closed high pressure vessels it was found that apart from the large-scale ridges, lean hydrocarbon–air flames may also exhibit cellular instability, provided the flame radius exceeds a certain critical value (Istratov & Librovich 1969; Groff 1982; figures 3 and 4). Under normal pressure an apparently similar mode of instability was observed in large-scale flames propagating from the centre of 5 and 10 m radius plastic bags, with cells reaching size *ca.* 10 cm (Lind & Whitson 1977).

It therefore seems safe to state that cellular instability is an inseparable feature of any premixed combustion. The size of the cells, however, is strongly dependent on the composition of the mixture, and in relatively small-scale systems the developed mode of the instability may well be obscured.

3. Premises of the theory

The principal difficulty in a theoretical approach to combustion processes is clearly the large number of elementary chemical reactions involved. Moreover, for many reactive mixtures of practical interest the pertinent knowledge of chemical kinetics is either not accurate enough or not yet available.

Fortunately, however, many aspects of the flame front dynamics may be described reasonably well without addressing the detailed chemistry, but rather using a naive one-step scheme:

$$\text{deficient reactant} \rightarrow \text{products} + \text{heat}, \tag{1}$$

coupled with the Arrhenius temperture dependence of the reaction rate.

The irrelevance of the chemical complexity is one of the miracles of premixed combustion and certainly a great blessing to the theoreticians whose analytical means are, as always, rather limited.

The basic mechanism of flame propagation is the successive ignition of a chemically

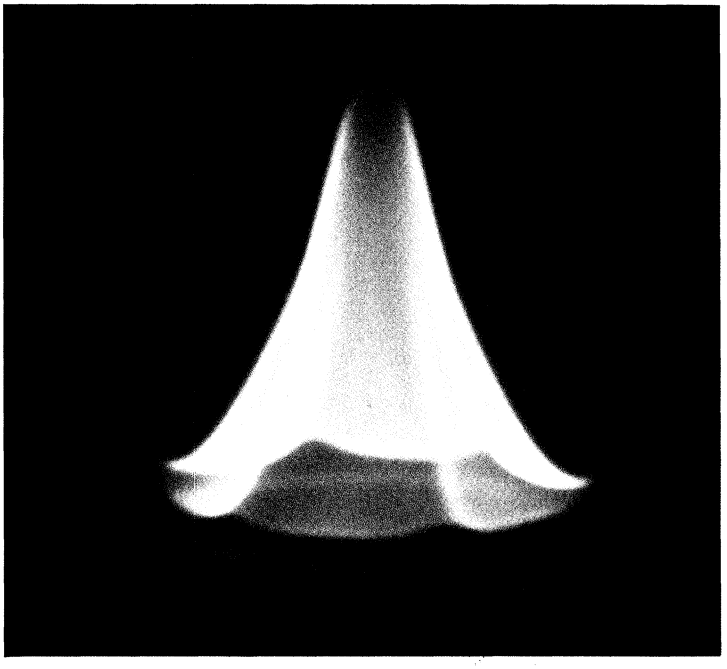

Figure 1. Polyhedral Bunsen burner flame of rich butane–air mixture.
(Courtesy of S. Sohrab; see also Jacobi & Sohrab 1990.)

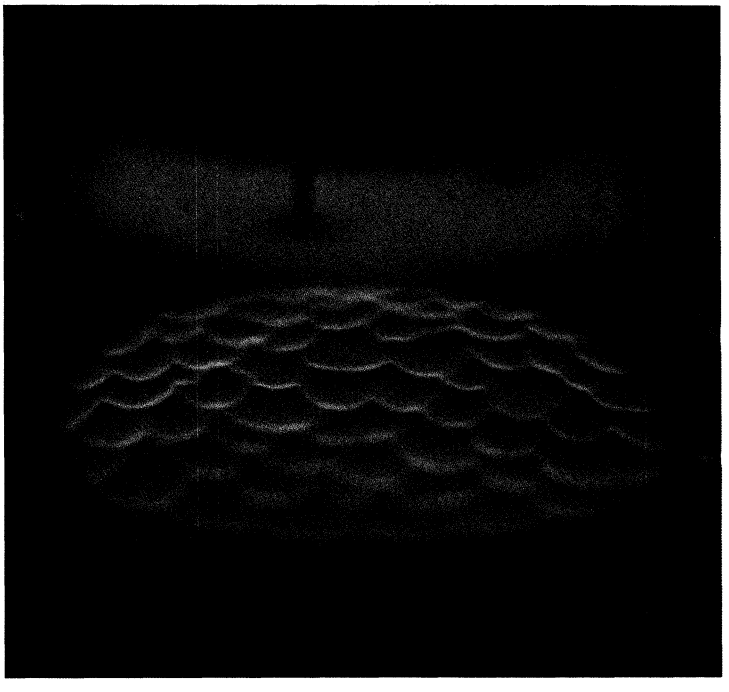

Figure 2. Rich propane–air cellular flame in state of chaotic self-motion.
(Courtesy of P. Clavin; see also Sabathier *et al.* 1981.)

PHILOSOPHICAL TRANSACTIONS OF THE ROYAL SOCIETY A MATHEMATICAL, PHYSICAL & ENGINEERING SCIENCES

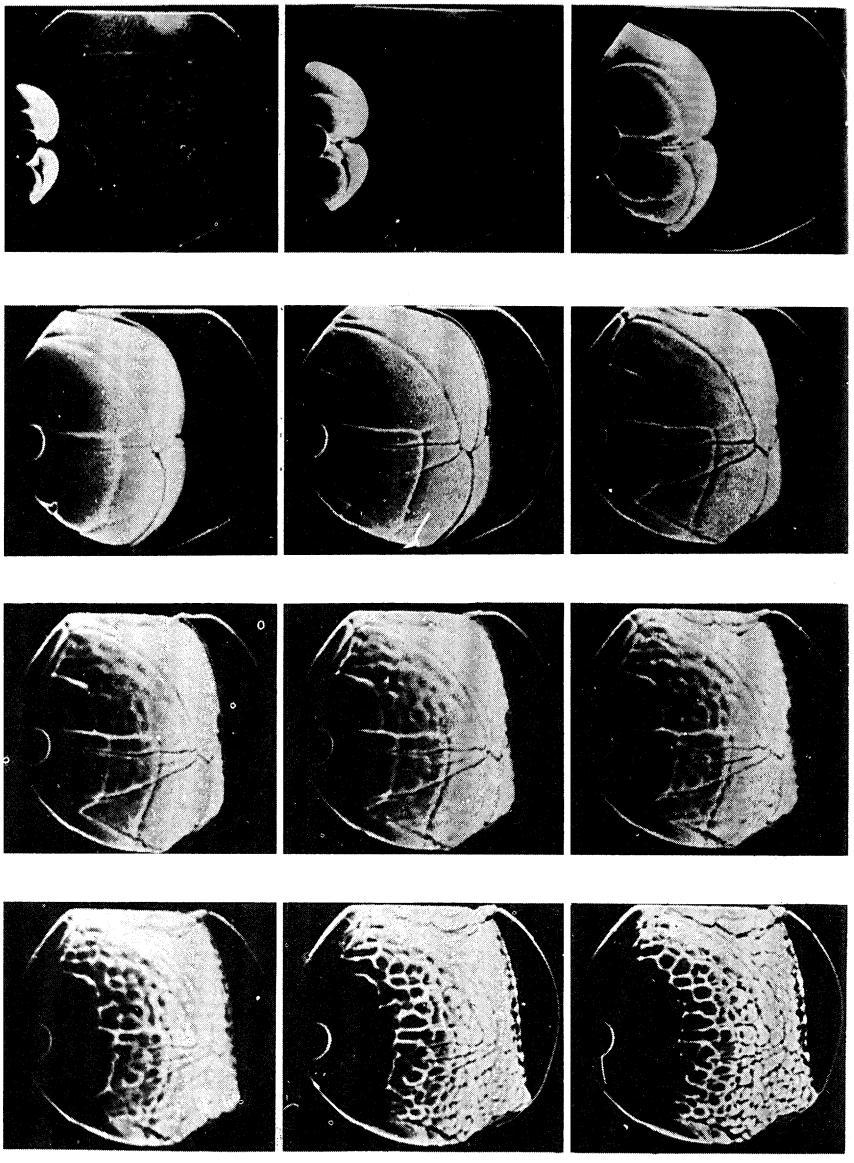

Figure 3. Successive frames showing spherical flame propagating in closed high-pressure vessel. Note large-scale ridges at the initial (non-cellular) stage of flame evolution. (Reproduced from Istratov & Librovich (1969), with permission.)

frozen explosive mixture by the heat liberated during the reaction. Typical profiles of temperature (T), concentration (C), and reaction rate ($W \approx C\exp(-E/RT)$) in a planar combustion wave are shown in figure 5. Here T_u is the temperature of the unburned cold mixture, at which the reaction rate is negligibly low; C_u is the initial concentration of the species which is entirely consumed in the reaction (deficient reactant); T_b is the adiabatic temperature of the burned gas, usually 5–10 times T_u; E is the activation energy of the reaction; R is the universal gas constant.

The thermal thickness (l_{th}) of the flame is defined as D_{th}/U_u, where D_{th} is the

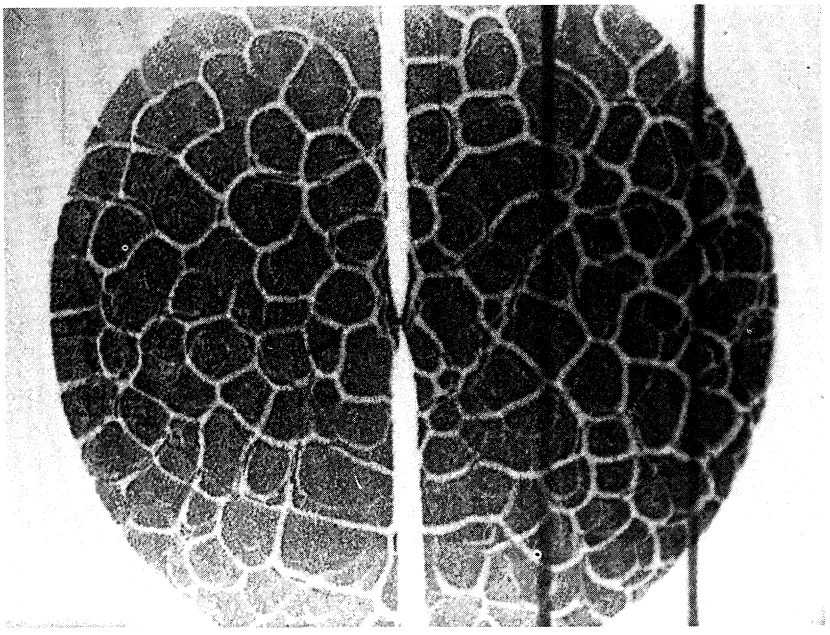

Figure 4. Photograph showing a cellular flame of lean propane–air mixture ignited at the centre of 260 mm diameter constant volume vessel. The initial pressure $P_0 = 400$ kPa, the initial temperature $T_0 = 300$ K, the equivalence ratio $\varphi = 0.80$. The picture corresponds to $t = 101$ ms from the moment of ignition (courtesy of E. G. Groff, originally in Groff 1982).

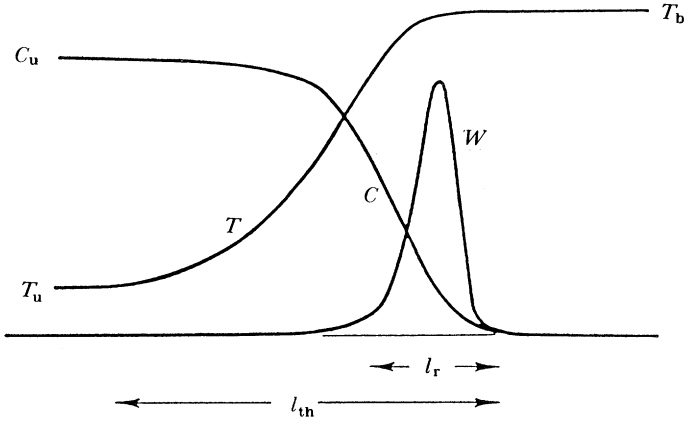

Figure 5. Profiles of temperature, concentration and reaction rate in a planar combustion wave.

thermal diffusivity of the mixture and U_u is the propagation speed of the planar flame relative to the unburned gas.

Because the reaction rate is strongly temperature dependent ($E/RT_b \approx 20$) the bulk of the chemical reaction occurs in a narrow temperature interval $\Delta T \approx RT_b^2/E$ around the maximum temperature T_b. This temperature interval corresponds to a thin layer of width $(RT_b/E)\, l_{th} = l_r$ (reaction zone), outside of which the reaction may be neglected.

The propagation speed of the flame (U_u) is determined by the balance between the heat liberated during the reaction and the heat required to preheat the fresh mixture

$$U_u = \left[\frac{2D_{th}}{T_b - T_u}\int_{T_u}^{T_b} W(C,T)\,dT\right]^{\frac{1}{2}} \tag{2}$$

(Zel'dovich & Frank-Kamenetsky 1938).

Due to its diffusive nature, the speed of flame spreading is significantly lower than the speed of sound. For one of the most rapidly burning mixtures ($2H_2+O_2$), $U_u \approx 10$ m s^{-1} and $l_{th} \approx 0.0005$ cm, while for one of the most slowly burning mixtures (6 % CH_4 + air), $U_u \approx 5$ cm s^{-1} and $l_{th} \approx 0.05$ cm.

In mathematical modelling, therefore, the effects of dynamic compressibility may often be neglected. If combustion occurs in an open space the density of the mixture may then be considered a function of temperature only.

Owing to the large activation energy, the reaction zone occupies only a narrow sublayer within the overall flame structure ($l_r \ll l_{th}$, figure 5). For planar or weakly distorted flames the reaction rate W may therefore be treated as a localized source distributed over a certain interface–flame front. Intensity of the source varies along the front as $\exp[E(T_f - T_b)/2RT_b^2]$ (cf. Sivashinsky 1975). Here T_f is the temperature at the curved front, which may differ from T_b by a quantity of the order of RT_b^2/E.

Due to the strong temperature dependence of the reaction rate, even slight changes in T_f may strongly affect its intensity, and thereby also local flame speed. The study of flame propagation is thus reduced to a free-boundary problem.

In suitably chosen non-dimensional variables and parameters the corresponding set of equations acquire the following compact form:

heat

$$\rho\frac{\partial\Theta}{\partial t} + \rho u_i\frac{\partial\Theta}{\partial x_i} = \frac{\partial}{\partial x_i}\frac{\partial\Theta}{\partial x_i} + e^{\frac{1}{2}\beta(\Theta-1)}\,\delta_F, \tag{3}$$

diffusion

$$\rho\frac{\partial C}{\partial t} + \rho u_i\frac{\partial C}{\partial x_i} = \frac{1}{Le}\frac{\partial}{\partial x_i}\frac{\partial C}{\partial x_i} - e^{\frac{1}{2}\beta(\Theta-1)}\,\delta_F, \tag{4}$$

continuity

$$\frac{\partial\rho}{\partial t} + \frac{\partial\rho u_i}{\partial x_i} = 0, \tag{5}$$

momentum

$$\frac{\partial\rho u_i}{\partial t} + \frac{\partial\rho u_i u_k}{\partial x_k} = -\frac{\partial p}{\partial x_i} + Pr\frac{\partial}{\partial x_k}\left(\frac{\partial u_i}{\partial x_k} + \frac{\partial u_k}{\partial x_i} - \tfrac{2}{3}\delta_{ik}\frac{\partial u_m}{\partial x_m}\right), \tag{6}$$

state

$$\rho = 1/(\sigma + (1-\sigma)\,\Theta). \tag{7}$$

Here $\delta_F = |\nabla F|\,\delta(F)$ is the surface delta-function localized along the front $F(x_i, t) = 0$. $F > 0$ corresponds to the unburned gas, while $F < 0$ corresponds to the burned gas.

The non-dimensional quantities in (3)–(7) are defined as follows: $\Theta = (T - T_u)/(T_b - T_u)$ is the reduced temperature; C is the concentration of the deficient reactant referred to C_u; ρ is the density referred to ρ_u, the density of the unburned gas; u_i is the gas velocity referred to U_u; p is the pressure referred to $\rho_u U_u^2$; x_i and t are the spatio-temporal coordinates referred to l_{th} and l_{th}/U_u respectively; Le is the Lewis number (the ratio of thermal diffusivity D_{th} to molecular diffusivity D_{mol}); Pr is the Prandtl number; $\beta = E(T_b - T_u)/RT_b^2$ is the Zeldovich number.

Far ahead of the flame front the reduced temperature Θ is zero, while the

concentration C is unity. Far beyond the front the temperature is equal to the adiabatic temperature of the combustion products, i.e. $\Theta = 1$. In the burned gas region ($F < 0$) the deficient reactant is completely consumed, i.e. $C \equiv 0$.

In this formulation the normal speed of the planar flame (U_u) is regarded as a prescribed physico-chemical parameter of the system.

4. Certain aspects of the linear stability analysis

In the frame of reference attached to the front, the planar ($F = x_3$) solution of (3)–(7) may be written as

$$\left.\begin{aligned} \Theta^{(0)} &= \exp x_3 \quad \text{for} \quad x_3 < 0, \\ \Theta^{(0)} &= 1 \quad \text{for} \quad x_3 > 0, \end{aligned}\right\} \tag{8}$$

$$\left.\begin{aligned} C^{(0)} = 1-[\Theta^{(0)}]^{Le}, \quad \rho^{(0)} &= [1+(1-\sigma)\,\Theta^{(0)}]^{-1}, \\ u_1^{(0)} = u_2^{(0)} = 0, \quad u_3^{(0)} &= 1+(1-\sigma)\,\Theta^{(0)}. \end{aligned}\right\} \tag{9}$$

For all the simplicity of the planar solution (8), (9) its linear stability analysis is far from trivial and has a long and bewildering history. There are, however, two limiting cases for which the problem is unlocked relatively easily. These are:

(i) first order long-wavelength approximation and

(ii) constant density approximation, $\sigma = 1$.

In the first limit the transport processes, and therefore the thermal-diffusive structure of the planar solution (8), (9), are irrelevant. Hence, the flame may be regarded as a discontinuity of density propagating relative to the non-viscous and non-conducting gas with a prescribed speed U_u.

Within the framework of this model, linear analysis of the stability of the plane flame front yields the following dispersion relation (Darrieus 1938; Landau 1944),

$$\omega = \frac{(\sigma+\sigma^2-\sigma^3)^{\frac{1}{2}}-\sigma}{\sigma(1+\sigma)}|\boldsymbol{k}|, \tag{10}$$

where $F = x_3 - \Phi(\boldsymbol{x}, t)$, $\Phi \approx \exp(\omega t + \mathrm{i}\boldsymbol{k}\cdot\boldsymbol{x})$, $\boldsymbol{x} = (x_1, x_2)$.

The rate of instability parameter ω is positive for all $\sigma < 1$. Thus, in the range of long-wavelength disturbances, thermal expansion exerts a destabilizing influence.

In the constant density limit thermal disturbances in the flame cannot be transformed into hydrodynamic disturbances, and so the problem of combustion proper is completely divorced from that of hydrodynamics. As a result, the stability problem becomes tractable for the whole range of wavenumbers. The pertinent dispersion relation, for the long-wavelength disturbances and $Le \approx 1$, yields (Barenblatt *et al.* 1962):

$$\omega = [\tfrac{1}{2}\beta(1-Le)-1]\,k^2 \quad (k = |\boldsymbol{k}|). \tag{11}$$

Flame stability thus appears to be quite sensitive to the composition of the mixture.

If the mobility of the deficient reactant is sufficiently high ($Le > Le_c = 1-2/\beta$), the flame is unstable, supporting the general tendency of the experimental observations.

In a typical flame, $\beta \approx 15$ and so $Le_c \approx 0.87$, which is quite a good threshold at least for lean hydrogen–air flames where $Le \approx 0.38$. The validity of this purely diffusive mechanism of instability for cellular flames of rich hydrocarbon–air mixtures is less obvious. As has been observed by Clavin & Williams (1982) (see also Frankel & Sivashinsky 1982; Pelce & Clavin 1982; Jackson & Kapila 1984), k^2-correction to the dispersion relation (10), incorporating dissipative effects, is

markedly affected by thermal expansion. As a result, for example, rich propane air flames appear to be thermo-diffusively stable ($Le > Le_c$) and in this sense formally indistinguishable from lean propane–air flames ($Le > 1$), although experimentally these systems behave quite differently.

One of the possible ways of resolving this difficulty is to account for heat loss. It has long been known (cf. Markstein 1949) that cellular structure in rich hydrocarbon–air mixtures has a tendency to occur near the flammability limit. As has been shown by Joulin & Clavin (1979) and by Sivashinsky & Matkowsky (1981), heat loss indeed expands the thermal-diffusive instability limits, moving Le_c to unity near the quenching point.

The alternative mechanism of cellular instability, proposed by Pelce & Clavin (1982), will be discussed in §8.

5. Nonlinear theory

As is suggested by the results of the linear analysis, near the stability threshold ($\sigma = 1$, $Le = Le_c$), the distorted flame front is expected to be both quasi-steady and quasi-planar, i.e. to evolve on time–length scales much larger than those inherent to the planar flame. Technically, this may lead to the separation of scales, and, thereby, to the lowering of the effective dimensionality of the underlying dynamical system. The pertinent nonlinear multiple-scale asymptotic analysis fully supported this idea, reducing the overall dynamical problem to the closed evolution for the interface itself (Sivashinsky 1977):

$$\Phi_t + \tfrac{1}{2}(\nabla\Phi)^2 + [\tfrac{1}{2}\beta(1-Le)-1]\,\nabla^2\Phi + 4\nabla^4\Phi = \tfrac{1}{2}(1-\sigma)\,I\{\Phi\}, \tag{12}$$

where

$$I\{\Phi\} = \frac{1}{4\pi^2}\int |\boldsymbol{k}|\, e^{i\boldsymbol{k}\cdot(\boldsymbol{x}-\boldsymbol{x}^*)}\,\Phi(\boldsymbol{x}^*, t)\,d\boldsymbol{x}^*\,d\boldsymbol{k}. \tag{13}$$

This equation is asymptotically exact when Le is close to Le_c, while σ is close to unity, i.e. when thermal expansion is considered to be weak.

To elucidate the role of each term in (12) it is useful to look at the dispersion relation corresponding to its linearized version

$$\omega = \tfrac{1}{2}(1-\sigma)\,k + [\tfrac{1}{2}\beta(1-Le)-1]\,k^2 - 4k^4. \tag{14}$$

The first term here clearly recovers the Darrieus–Landau relation (10) for $\sigma \approx 1$, while the second, thermal-diffusive instability (11). The third term yields dissipation of short-wavelength disturbances, thereby providing the smoothness of the nonlinear evolution. Due to this term there is always a wavelength $\lambda_c = 2\pi/k_c$ corresponding to the maximum amplification rate ($\max \omega$) of small harmonic disturbances.

The nonlinear term in (12) relates to the small deviation of the front normal from the axis x_3. This nonlinearity, for all its simple kinematic origin, proves to be quite sufficient not only in restraining the otherwise exponentially growing modes, but also in providing mode coupling leading to the self-turbulization of the system. To clarify the individual impacts of thermal-diffusive and of hydrodynamic instability on flame dynamics, it is instructive to study two versions of (12): one in which hydrodynamic instability is completely suppressed,

$$\Phi_t + \tfrac{1}{2}(\nabla\Phi)^2 + [\tfrac{1}{2}\beta(1-Le)-1]\,\nabla^2\Phi + 4\nabla^4\Phi = 0 \tag{15}$$

PHILOSOPHICAL TRANSACTIONS OF THE ROYAL SOCIETY A MATHEMATICAL, PHYSICAL & ENGINEERING SCIENCES

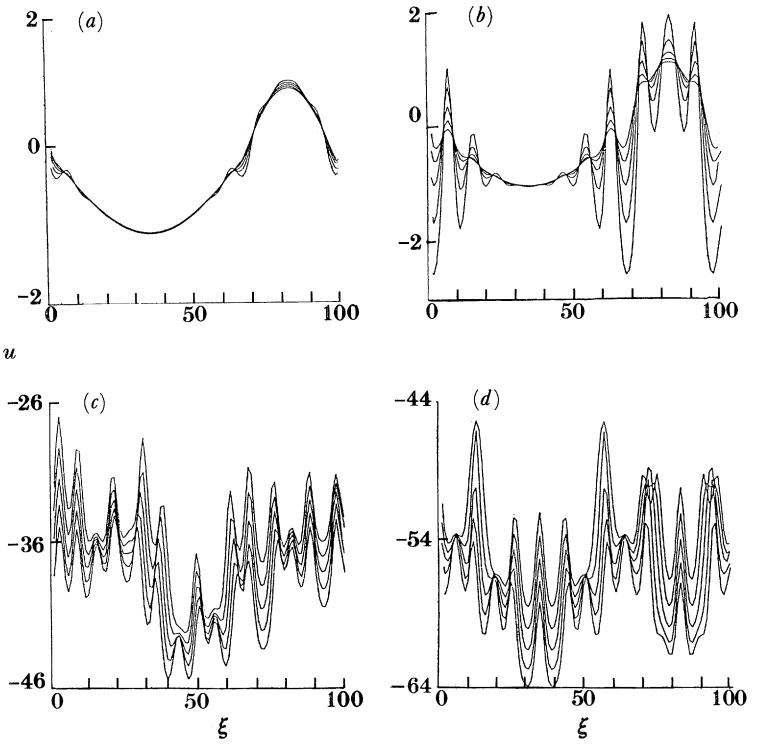

Figure 6. Thermal-diffusive instability. Numerical solution of the equation $u_\tau+\frac{1}{2}(u_\xi)^2+u_{\xi\xi}+u_{\xi\xi\xi\xi}=0$ (rescaled one-dimensional version of (15)) on the interval $10\lambda_c$ with periodic boundary conditions. Each frame represents the configurations of the flame front at five consecutive equidistant instants of time. (*a*) Flame front close to the moment of initial disturbance; (*b*) formation of quasi-periodic cellular structure; (*c*) and (*d*) flame front in developed self-turbulent régime. (Michelson & Sivashinsky 1977.)

and the second, in which thermo-diffusive instability is absent ($Le > Le_c$), and, therefore, it is presumably safe to omit the fourth-order dissipation term. Hence,

$$\Phi_t+\tfrac{1}{2}(\nabla\Phi)^2+[\tfrac{1}{2}\beta(1-Le)-1]\nabla^2\Phi=\tfrac{1}{2}(1-\sigma)I\{\Phi\}. \tag{16}$$

6. Thermal-diffusive instability: numerical experiments

Numerical experiments with (15), which at $Le < Le_c$ describes purely thermal-diffusive flame instability, show that when a planar front is disturbed it evolves ultimately into a cellular pattern with a cell size close to λ_c.

The striking feature of (15) is that the cellular structure it generates appears to be essentially non-steady, the cells being in a state of continuous irregular self-motion (figures 6 and 7). Different initial conditions generate different solutions. However, with elapsing time these solutions become statistically indistinguishable. Thus, being quite deterministic in nature, equation (15) appears to be capable of displaying turbulence-type behaviour; still rather a rare feature in classical phenomenology. It is interesting that the chaotic self-motion in cellular flames is long known from experiments (Markstein 1949, 1951) and was later reconfirmed in a study by Sabathier *et al.* (1981) under carefully controlled flow conditions (figure 2).

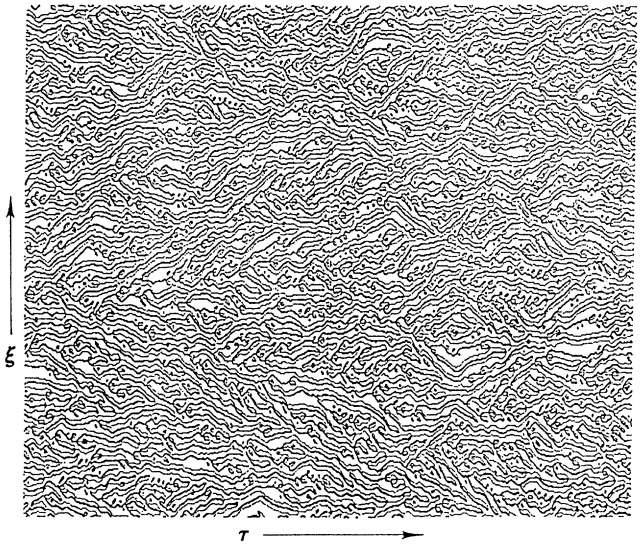

Figure 7. Thermal-diffusive instability. Numerical solution of the one-dimensional version of (15), showing spatio-temporal evolution of the maxima and minima of the self-fluctuating cellular structure. The problem was solved on the interval $50\lambda_c$ with periodic boundary conditions (courtesy of H. Chaté; see also Chaté 1989).

The temperature variation over the front predicted by the theory also correlates well to the observations yielding a higher temperature at the troughs and lower at the crests of the cell,

$$\Theta - 1 \approx (Le - 1)\,\nabla^2 \Phi \text{ at the front.} \tag{17}$$

However, as has already been mentioned, quantitative correlation here is likely only for lean hydrogen–air flames, unless the effects of heat loss are taken into account.

Recently Denet (1989) and Denet & Handelwang (1990) (see also Patnaik *et al.* 1988) undertook a direct numerical simulation of cellular instability based on the constant density reaction–diffusion system with the distributed reaction rate W. They found that close to the stability threshold the reaction wave indeed evolves according to the predictions of the flame equation (15) (see figure 8).

However, sufficiently far from the bifurcation point the cellular flame quenches at the crests resulting in a complete disintegration of the front. An apparently similar phenomenon was recently observed by Ronney (1990) in his zero-gravity experiments with lean hydrogen–air flames.

To conclude this section we would like to make one remark concerning the high activation energy limit and the associated δ-function approximation for the reaction rate.

For the actual derivation of (16) the high activation energy assumption is quite helpful technically. Yet, as has been demonstrated by Kuramoto (1980), due to the slowly varying structure of the reaction wave, this requirement may well be relaxed without affecting the basic nature of the evolution.

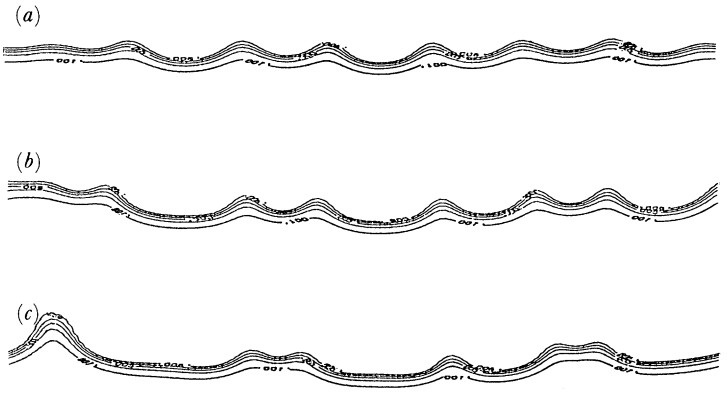

Figure 8. Distribution of isotherms in a chaotically evolving cellular flame at three distinct moments of time. Numerical solution of the constant-density reaction–diffusion model for premixed flame propagation. The aspect width of the systems is $120l_{\rm th}$; $W \approx C\exp(-E/RT)$; $T_{\rm u}/T_{\rm b} = 0,2$; $Le = 0.6$; $\beta = 10$ (courtesy of B. Denet and P. Handelwang; originally in Denet (1989)). (*a*) $t = 48$, (*b*) $t = 72$, (*c*) $t = 96$.

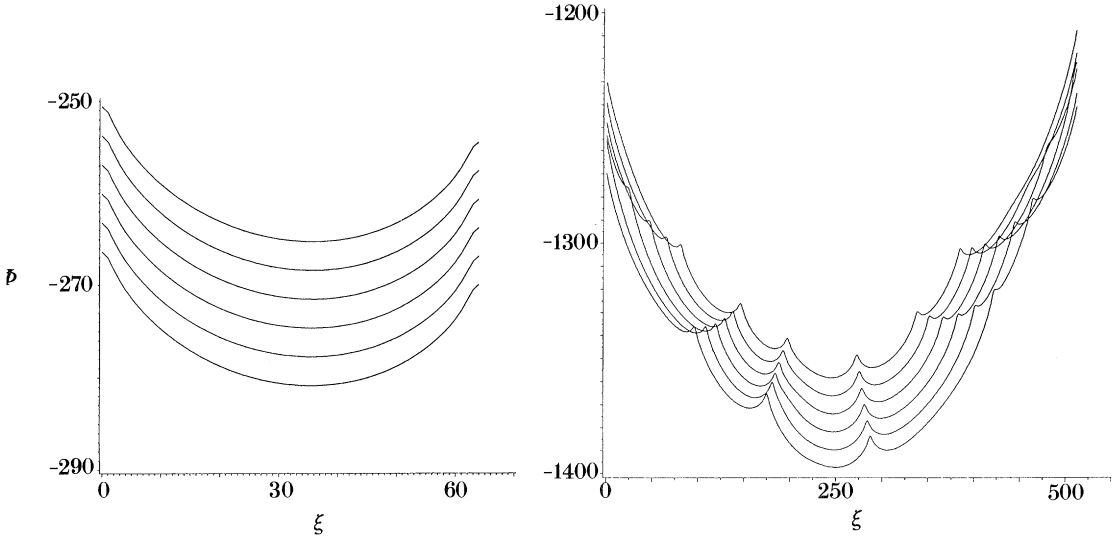

Figure 9. Hydrodynamic instability. Numerical solution of the equation

$$\Phi_\tau + \tfrac{1}{2}(\Phi_\xi)^2 = \Phi_{\xi\xi} + \tfrac{1}{2}I\{\Phi\}$$

(rescaled one-dimensional version of (16)) on the intervals of (*a*) $2.5\lambda_{\rm c}$ and (*b*) $20\lambda_{\rm c}$, with adiabatic boundary conditions (Gutman & Sivashinsky 1990).

7. Hydrodynamic instability: numerical experiments

The typical length scale of the cellular structure ($\lambda_{\rm c}$) induced by (15) correlates well with the predictions of the linear theory. In the case of hydrodynamic instability described by (16), it would be natural to expect a similar correlation. Numerical experiments show, however, that here the situation is much more complicated and strongly depends on the size of the domain.

At moderately wide intervals (*ca.* $10\lambda_{\rm c}$) the one-dimensional version of (16), solved

subject to periodic boundary conditions, yields a single cusp-like configuration, whose location depends on the initial data. For more realistic, adiabatic, boundary conditions the crest of the final cusp never settles down inside the interval, rather being attracted to one (or both) of its ends. As a result the equilibrium flame shape appears as a smooth surface convex toward the fresh mixture (figure 9*a*).

The very early stage of the flame evolution basically follows the indications of the linear analysis; modes corresponding to λ_c have the highest growth rate. This, however, does not last long. The initially appearing small-scale cells merge, forming bigger cells and so on until the large single cell filling up all the interval is finally formed. After this, the flame configuration settles down as a completely time independent progressive wave (Michelson & Sivashinsky 1977; Denet 1989; Gutman & Sivashinsky 1990). The convex flame configuration generates a gradient in the tangential component of the gas velocity along the front, stretching out ever present small disturbances. This is apparently the reason for its remarkable stability (Zel'dovich *et al.* 1980*b*).

The source of the Darrieus–Landau paradox, therefore, is a complete linearization of the evolution equations. The nonlinearity brings in a major stabilizing factor, sustaining smooth configurations on scales considerably exceeding λ_c, suggested by the linear theory.

However, at rather wider intervals ($20\lambda_c$) the stabilizing effect of stretching is weakened, and the basic convex configuration acquires a fine structure comprising of time-dependent smaller scale cells (figure 9*b*). The cells being in a state of permanent splitting and merging move from the trough of the basic large scale configuration to its crest or to the ends of the interval (Michelson & Sivashinsky 1982; Gutman & Sivashinsky 1990). Here the cells may often reach the size *ca.* $5\lambda_c$. The dual nature of hydrodynamic instability is likely to be related to similar observations made for high-pressure lean hydrocarbon–air flames (Istratov & Librovich 1969; Groff 1982; figures 3 and 4). In these systems all scales are proportionally reduced and the secondary structure becomes quite observable in the laboratory.

Interestingly enough, the found non-steady cellular structure does not seem to be admissible by the pole-decomposition theory of (16) recently proposed by Thual *et al.* (1985) and Joulin (1989). Since at wide intervals larger-scale configuration appear to be rather sensitive to small perturbations, it is argued that numerically (and presumably experimentally) observed small-scale cells are actually induced by weak external (e.g. numerical) noise rather than a self-sustaining phenomena (Joulin 1989). It would be important, therefore, to ascertain whether the class of meramorphic functions associated with the pole-decomposition approach is indeed wide enough to embrace all the relevant solutions, or whether the matter is more involved.

8. Effects due to acceleration

Since combustion is accompanied by thermal expansion of the gas, it is clear that buoyancy will exert a stabilizing influence on downward propagating flames. This problem has been studied by Pelce & Clavin (1982).

In contradistinction to a freely propagating flame, a flame moving in the presence of a stabilizing acceleration is stable to longwave disturbances. Near the stability threshold the unstable modes are concentrated near λ_c (the wavelength corresponding to the maximum amplification rate ω). As a result one may observe λ_c-size cells even in small-scale systems which are thermo-diffusively stable. Pelce &

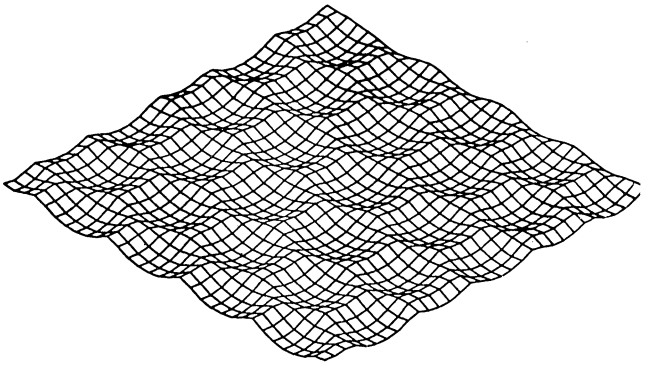

Figure 10. Thermal expansion induced hexagonal cellular structure occurring near the stability threshold ($G = 0.8G_c$). Numerical solution of (18) in $5\lambda_c \times 5\lambda_c$ square with periodic boundary conditions (Michelson & Sivashinsky 1982).

Clavin (1982) argue that this mechanism may be the reason for cellular instability observed in rich propane–air flames in vertical tubes (figure 2). To clarify the matter the appropriate zero-gravity experiments would be very instructive.

With regards to the nonlinear dynamics, the corresponding evolution equation incorporating both the Darrieus–Landau instability (10) and the stabilizing effect of buoyancy may be written as (cf. Michelson & Sivashinsky 1982; Rakib & Sivashinsky 1987)

$$\Phi_t + \tfrac{1}{2}(\nabla\Phi)^2 + [\tfrac{1}{2}\beta(1-Le)-1]\nabla^2\Phi + G[\Phi - \langle\Phi\rangle] = \tfrac{1}{2}(1-\sigma)I\{\Phi\}, \tag{18}$$

where $G = \frac{1}{2}g(1-\sigma)l_{\rm th}U_n^{-2}$ is the non-dimensional acceleration; $\langle\ldots\rangle$ means average over the tube cross-section.

For $G > G_c = \frac{1}{16}(1-\sigma)^2[\frac{1}{2}\beta(Le-1)+1]^{-1}$ the planar flame is linearly stable. However, at G somewhat below G_c the solution of (18) assumes a cellular structure which may be chaotic or even regular, provided G is close enough to G_c (figure 10).

9. Concluding remarks

1. Despite the limited range of its strict validity, equation (12) appears to be rich enough to cover rather a wide spectrum of phenomena apparently pertinent to the main features of real premixed flames. Even considering all the information available on (12) there is still much to be done in answering some very basic questions. For example, how does the overall speed of the wrinkled flame depend on the length of the interval? Does it grow indefinitely with the interval length, or approach a certain finite limit? Some large-scale numerical studies here would be quite welcome.

2. Equation (12) being associated with small disturbances of the planar front ($x_3 = 0$), somewhat conceals the geometrical nature of the terms it is comprised of.

As has been recently shown by Frankel & Sivashinsky (1988) and Frankel (1990*a*), in the geometrically invariant formulation (12) is modified to

$$\boldsymbol{n}\cdot\mathrm{d}\boldsymbol{r}/\mathrm{d}t = 1 + [\tfrac{1}{2}\beta(1-Le)-1]\kappa + 4\nabla_S^2\kappa + w_n, \tag{19}$$

where $\boldsymbol{r}$ is the position of the flame interface S; $\boldsymbol{n}$ is the outward normal; $\kappa = \nabla\cdot\boldsymbol{n}$ is the curvature; $\nabla_S^2\kappa$ is the Laplace–Beltrami operator (surface laplacian) of the

curvature (in the two-dimensional case $\nabla_S^2 \kappa = \kappa_{ss}$, where s is the arc length of the front curve);

$$w_n(\boldsymbol{r}) = \frac{(1-\sigma)}{2}\left[1 + \frac{\boldsymbol{n}}{(\nu-1)\,\pi} \cdot \int_S \frac{(\boldsymbol{r}-\xi)}{|\boldsymbol{r}-\xi|^\nu} \mathrm{d}s\right] \tag{20}$$

is the normal projection of the gas velocity induced by thermal expansion (Frankel 1990*a*); $\nu\,(=2$ or $3)$ is the dimension of the system.

3. The combustion systems discussed in this paper, for all their fundamental interest, are rather idealized in nature. Flame propagation problems of practical interest deal as a rule with situations where the overall system is confined and subject to the influence of external sources (or sinks) of energy, species as well as momentum. A vast experimental and theoretical data is accumulated on these aspects of premixed combustion and could claim at least as much right of attention as those who received their due here.

With regard to spontaneous flame instability, perhaps the most serious omission is the absence of any discussion of the oscillatory and spinning modes of flame propagation which are expected to emerge in high Lewis number flames. Despite a rather scanty experimental data on the phenomena in gaseous premixtures, in the combustion of some condensed system, where $Le = \infty$, this mode of instability appears to be quite feasible and received a good deal of attention both experimentally and theoretically.

Similar to the gaseous systems one can obtain here an approximate closed equation for the flame interface (Frankel 1990*b*). Moreover, as has been recently found by Bayliss & Matkowsky (1990), the oscillatory instability appears to be rich enough to exhibit not only regular periodic pulsations but the irregular chaotic pulsations as well.

These studies were supported by the U.S. Department of Energy under Grant no. DEFG02-88ER13822, by the National Science Foundation under Grants nos CTS-8910903 and DMS-8802596, and by the U.S. Air Force Office at Scientific Research under Grant no. AFOSR-88-103, while the author was visiting the Institute for Applied Mathematics & Scientific Computing of Indiana University, Bloomington.

The warm hospitality of Professor R. Temam is greatly appreciated.

References

Barenblatt, G. I., Zel'dovich, Y. B. & Istratov, A. G. 1962 *Zh. Prikl. Mekh. Tekh. Fiz.* **4**, 21–26.

Bayliss, A. & Matkowsky, B. J. 1990 Two routes to chaos in solid fuel combustion. *SIAM J. appl. Math.* **50**, 437–459.

Buckmaster, J. & Ludford, G. S. S. 1982 *Theory of laminar flames*. Cambridge University Press.

Chaté, H. 1989 Thése de l'Université Pierre et Marie Curie, Paris, France.

Clavin, P. 1985 *Prog. Energy & Combust. Sci.* **11**, 1–59.

Clavin, P. & Williams, F. A. 1982 *J. Fluid Mech.* **116**, 251–282.

Darrieus, G. 1938 Propogation d'un front de flamme: assai de théorie des vitesses anomales de déflagration par developpement spontané de la turbulence. (Presented at the Sixth International Conference of Applied Mechanics, Paris, 1946.)

Denet, B. 1989 Thése de l'Université de Provence, Marseille, France.

Denet, B. & Handelwang, P. 1990 A pseudo-spectral scheme for turbulent thermo-diffusive premixed flames. (Submitted.)

Frankel, M. L. 1990*a* An equation of surface dynamics modelling the thermal-expansion driven flame fronts. *Phys.* Fluids. (In the press.)

Frankel, M. L. 1990*b* On the equation of pulsating flame fronts in solid fuel combustion. *Physica* D. (In the press.)

Frankel, M. L. & Sivashinsky, G. I. 1982 *Combust. Sci. Tech.* **29**, 207–244.

Frankel, M. L. & Sivashinsky, G. I. 1988 *Physica* D **30**, 28–42.

Groff, E. G. 1982 *Combust. Flame* **48**, 51–52.

Gutman, S. & Sivashinsky, G. I. 1990 The cellular nature of hydrodynamic flame instability. *Physica* D. (In the press.)

Hohenberg, P. C. & Shraiman, B. I. 1989 *Physica* D **37**, 109–115.

Istratov, A. G. & Librovich, A. B. 1969 *Astronaut. Acta* **14**, 453–467.

Jackson, T. L. & Kapila, A. K. 1984 *Combust. Sci. Tech.* **41**, 191–201.

Jacobi, A. N. & Sohrab, S. H. 1990 Chemical kinetics and thermal aspects of cellular premixed flames. *Combust. Sci. Tech.* **69**, 17–32.

Joulin, G. 1989 *J. Physique* **50**, 1069–1072.

Joulin, G. & Clavin, P. 1979 *Combust. Flame* **35**, 139–153.

Kuramoto, Y. 1980 *Prog. theor. Phys.* **63**, 1885–1903.

Landau, L. D. 1944 *Acta Physicochim. URSS* **19**, 77–85.

Lind, C. D. & Whitson, J. 1977 Phase II Report No. CG-D-85-77 Department of Transportation, U.S. Coast Guard Final Report, ADA 047585.

Manneville, P. 1988 In *Propagation in systems far from equilibrium* (ed. J. E. Wesfreid). Berlin: Springer-Verlag.

Markstein, G. H. 1949 *J. chem. Phys.* **17**, 428–429.

Markstein, G. H. 1951 *J. aeronaut. Sci.* **18**, 199–209.

Markstein, G. H. 1964 *Nonsteady flame propagation*. Oxford: Pergamon.

Michelson, D. M. & Sivashinsky, G. I. 1977 *Acta Astronaut.* **4**, 1207–1221.

Michelson, D. M. & Sivashinsky, G. I. 1982 *Combust. Flame* **48**, 211–217.

Patnaik, G., Kailasanath, R., Laskey, K. J. & Oran, E. S. 1988 In *Proc. 22nd Symp. (Int.) Combust.* Pittsburg, Pennsylvania: The Combustion Institute.

Pelce, P. & Clavin, P. 1982 *J. Fluid Mech.* **124**, 219–237.

Rakib, Z. & Sivashinsky, G. I. 1987 *Combust. Sci. Tech.* **54**, 69–84.

Ronney, P. 1990 Near-limit flame structure at low Lewis number. *Combust. Flame*. (In the press.)

Sabathier, F., Boyer, L. & Clavin, P. 1981 *Prog. Astronaut. Aeronaut.* **76**, 246–258.

Sivashinsky, G. I. 1975 *J. chem. Phys.* **62**, 638–643.

Sivashinsky, G. I. 1977 *Acta Astronaut.* **4**, 1177–1206.

Sivashinsky, G. I. 1983 *A. Rev. Fluid Mech.* **15**, 179–199.

Sivashinsky, G. I. & Matkowsky, B. J. 1981 *SIAM J. appl. Math.* **40**, 255–260.

Smith, F. A. & Pickering, S. F. 1928 *Ind. Engng Chem.* **20**, 1012–1013.

Smithells, S. & Ingle, K. 1882 *J. chem. Soc.* **61**, 204–217.

Strehlow, R. A. 1984 *Combustion fundamentals*. New York: McGraw-Hill.

Thual, O., Frisch, U. & Henon, M. 1985 *J. Physique* **46**, 1485–1494.

Williams, F. A. 1985 *Combustion theory*. New York: Benjamin/Cummings.

Zel'dovich, Y. B. 1944 *Theory of combustion and detonation of gases*. Acad. Sci. USSR. (In Russian.)

Zel'dovich, Y. B. & Frank-Kamenetsky, D. A. 1938 *Acta Physicochim. URSS* **9**, 341–350.

Zel'dovich, Y. B., Istratov, A. G., Kidin, N. I. & Librovich, V. B. 1980*b* *Combust. Sci. Tech.* **24**, 1–13.

Zel'dovich, Y. B., Barenblatt, G. I., Librovich, V. B. & Makhviladze, G. M. 1980*a* *Mathematical theory of combustion and explosion*. Moscow: Nauka. (In Russian.)

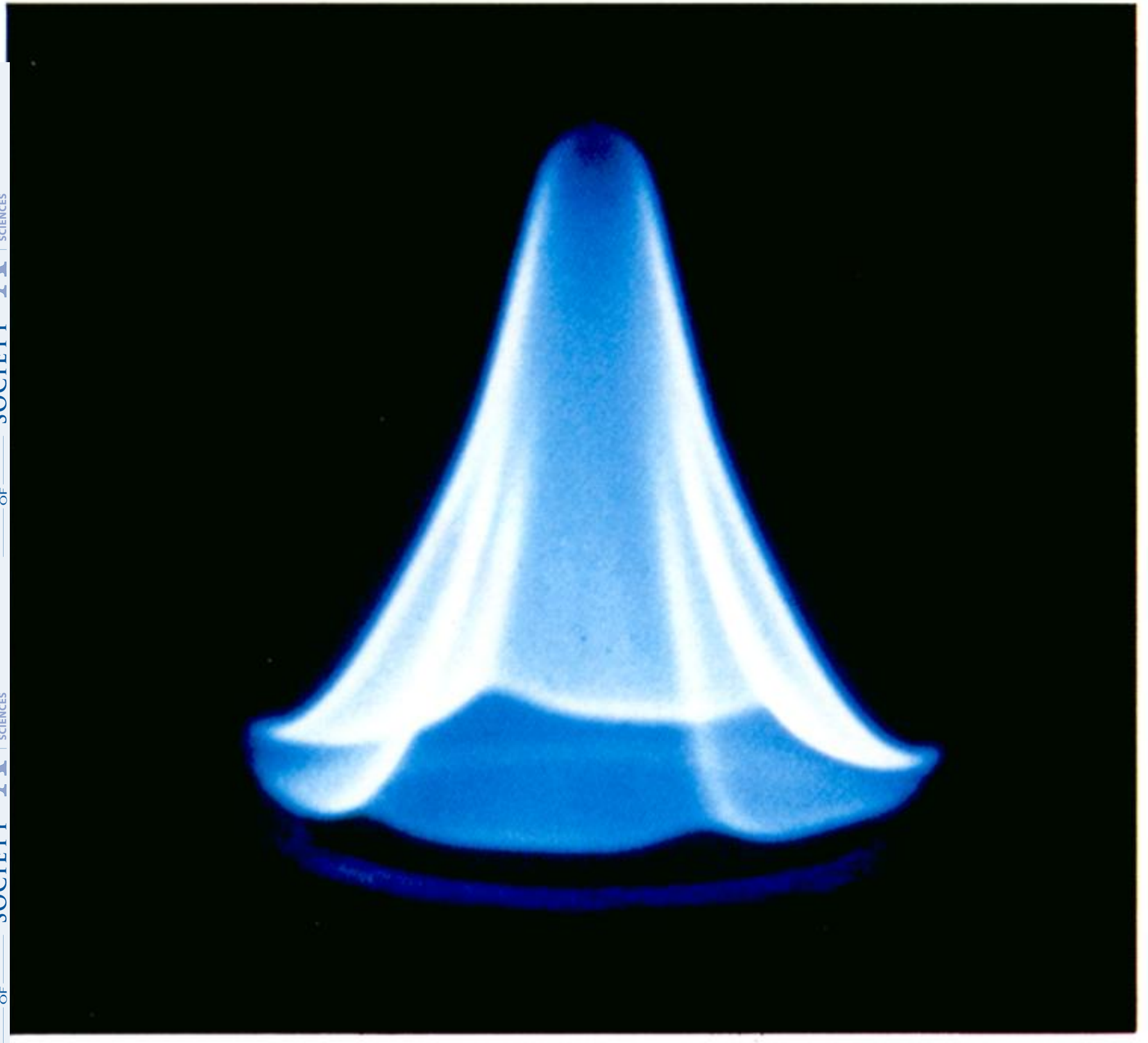

gure 1. Polyhedral Bunsen burner flame of rich butane–air mixture. (Courtesy of S. Sohrab; see also Jacobi & Sohrab 1990.)

PHILOSOPHICAL TRANSACTIONS OF THE ROYAL SOCIETY A MATHEMATICAL, PHYSICAL & ENGINEERING SCIENCES

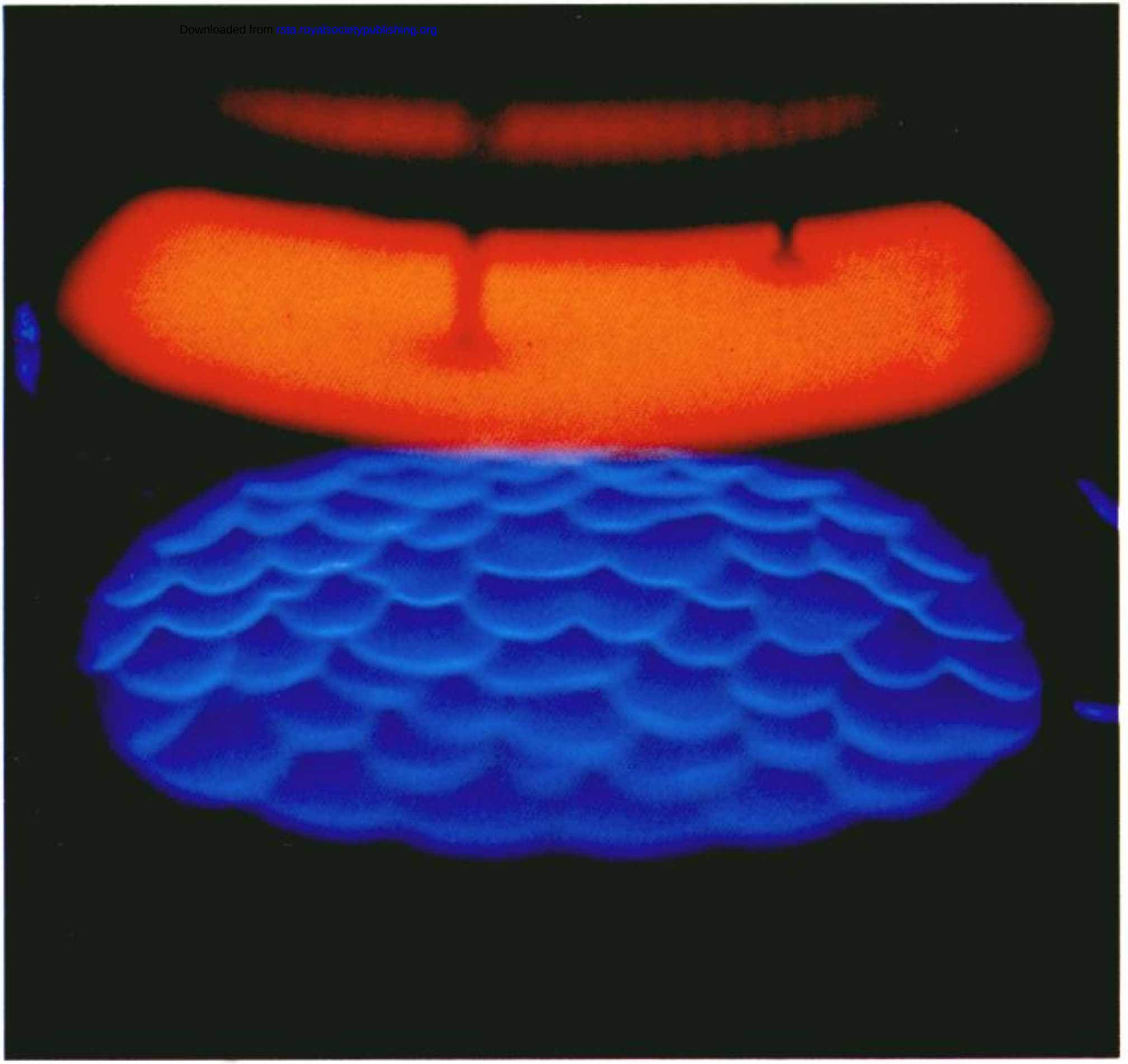

gure 2. Rich propane–air cellular flame in state of chaotic self-motion. (Courtesy of P. Clavin; see also Sabathier *et al.* 1981.)

PHILOSOPHICAL TRANSACTIONS OF THE ROYAL SOCIETY A MATHEMATICAL, PHYSICAL & ENGINEERING SCIENCES

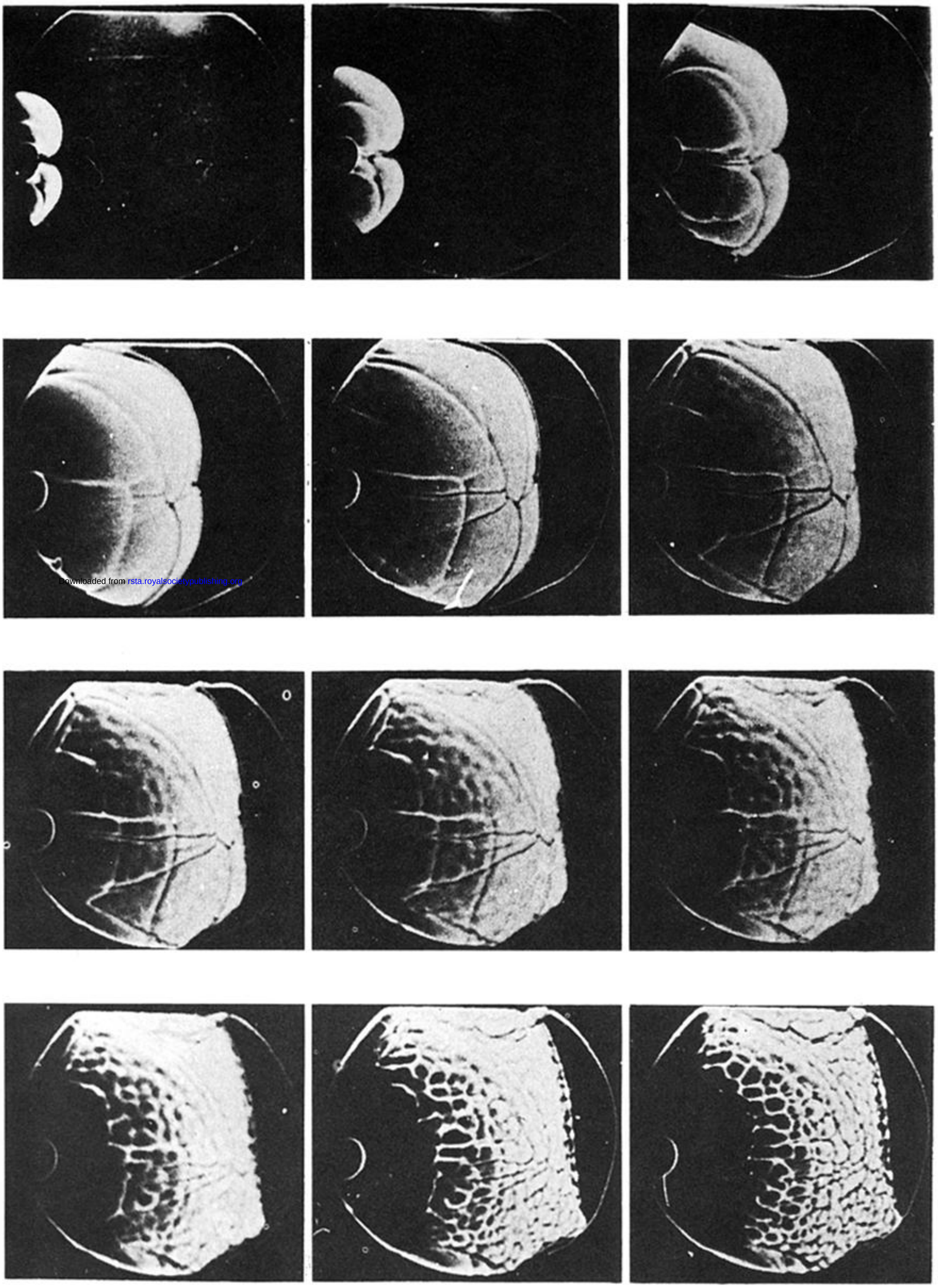

igure 3. Successive frames showing spherical flame propagating in closed high-pressure vessel. ote large-scale ridges at the initial (non-cellular) stage of flame evolution. (Reproduced from tratov & Librovich (1969), with permission.)

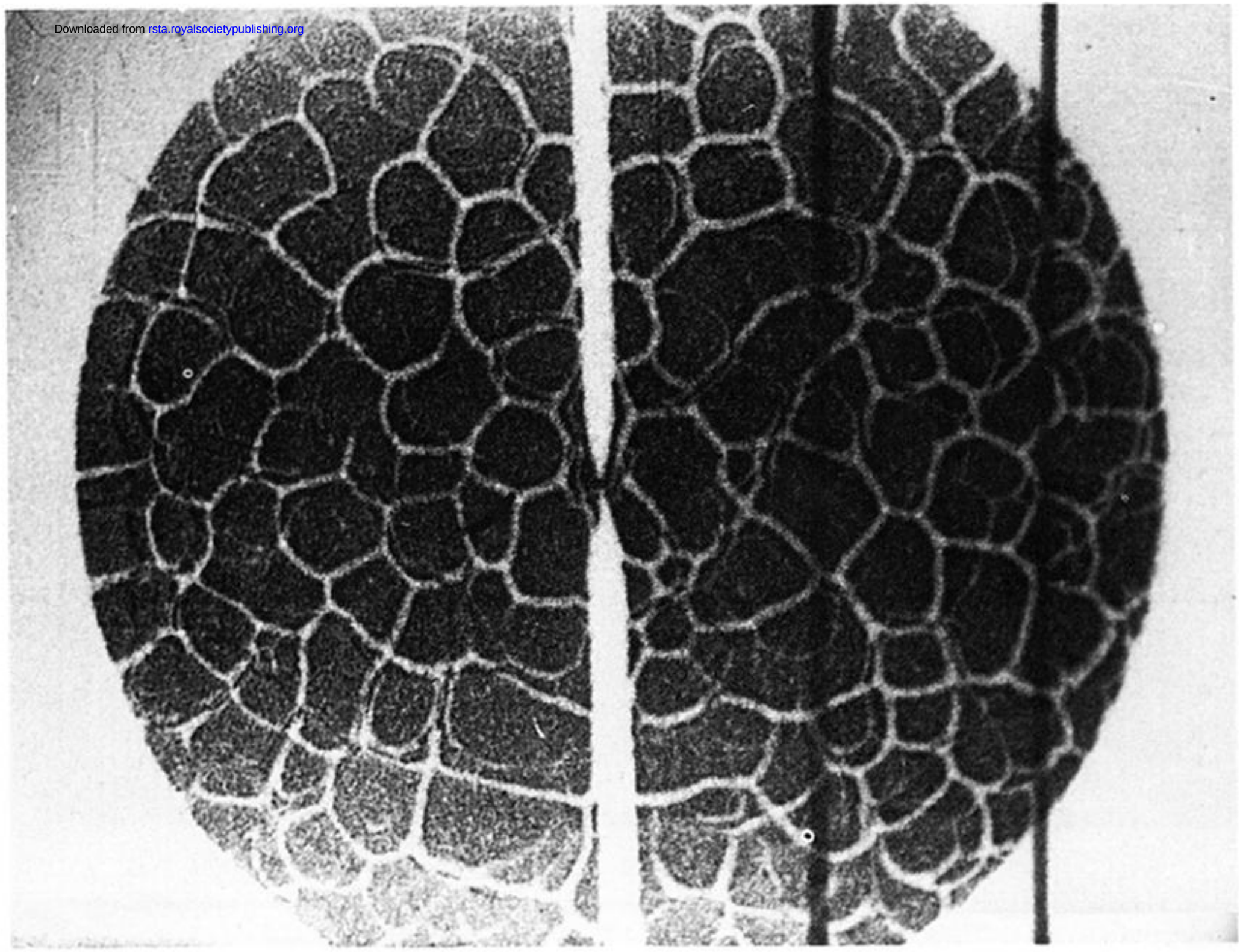

gure 4. Photograph showing a cellular flame of lean propane–air mixture ignited at the centre of 50 mm diameter constant volume vessel. The initial pressure $P_0 = 400$ kPa, the initial temperature = 300 K, the equivalence ratio $\varphi = 0.80$. The picture corresponds to $t = 101$ ms from the oment of ignition (courtesy of E. G. Groff, originally in Groff 1982).